30th Eurosensors Conference, EUROSENSORS 2016

# Understanding the behavior of stimuli-response ionogels for microfluidic applications

Nerea Gil-González[1], T. Akyazi[2,3], A. Zuzuarregui[4], E. Castaño[1], F. Benito-Lopez[3,5], M.C. Morant-Miñana[4]*

*1. CEIT and Tecnun (University of Navarra), Donostia-San Sebastián, Spain*
*2. Tecnun (University of Navarra), Donostia-San Sebastián, Spain*
*3. Analytical Microsystems & Materials for Lab-on-a-Chip (AMMa-LOAC) Group, Microfluidics UPV/EHU Cluster, Analytical Chemistry Department, University of the Basque Country UPV/EHU, Vitoria-Gasteiz, Spain*
*4. CIC nanoGUNE Consolider, Donostia-San Sebastián, Spain*
*5. Insight: Centre for Data Analytics, National Centre for Sensor Research, Dublin City University, Dublin, Ireland*

**Abstract**

Electrochemical Impedance Spectroscopy (EIS) studies of two different ionogels (IOs) are performed using gold interdigitated electrodes (Au-IDEs). Poly(N-isopropylacrylamide) (pNIPAAM) is polymerized in the presence of two ionic liquids (ILs), ethyl-3-methylimidazolium ethyl sulfate [$C_2$mIm][$EtSO_2$] (1) or trihexyltetradecyl-phosphonium dicyanamide [$P_{6,6,6,14}$][DCA] (2). The Nyquist diagrams of the IOs reflect significant differences due to their polarity and porosity dissimilarities. This fact is supported with the study of the diffusion of water through the polymer matrix, which is faster for IO-1, the most porous IO. Moreover, the ability of IO-1 and IO-2 to conduct current is measured and the sheet resistance of IO-2 is two orders of magnitude higher than IO-1. Finally, the swelling/drying properties of the IOs are monitored exposing them to several vacuum and rehydration cycles. The Nyquist plot of IO-1 shows faster diffusion and recovery of the original properties. Both hydrophilicity and porosity are in the basis of this result.

Peer-review under responsibility of the organizing committee of the 30th Eurosensors Conference.

Keywords: Ionogel (IO); Electrochemical Impedance Spectroscopy (EIS); Interdigitated Electrodes (IDEs); smart materials; ionic liquid (IL)

## 1. Introduction

Smart materials are systems that integrate several functions that respond repetitively to external stimuli. Often the response can be a reversible conformational change making them suitable to control, for example, microfluidic devices [1]. In this context IOs are a new class of hybrid materials, in which a polymer gel incorporates an IL as

* Corresponding author. Tel.: +34 943 57 40 00; fax: +0-000-000-0000 .
*E-mail address:* mc.morant@nanogune.eu


Peer-review under responsibility of the organizing committee of the 30th Eurosensors Conference.

solvent. These materials swell in an aqueous environment and shrink with an environmental stimuli (magnetic, thermal, light, pH or electrochemical) depending on the switchable functional group attached to the gel network [2][3]. IOs are promising materials for a broad range of applications such as microfluidic valves for the automatic regulation of a flow [4], drug delivery systems [5] and sensors. Electrochemical sensors are widely used for detection of a wide range of analytes. The success of many of these sensors is governed by the condition and stability of the membrane/electrode surface. Understanding and manipulating these interfacial processes has assisted in the development of membranes/electrodes with new and improved response characteristics. EIS has been used to provide information on various fundamental processes (i.e., adsorption/film formation, rate of charge transfer, ion exchange, diffusion, etc.) that occur at the electrode–electrolyte interface [6]. In the present work we report the EIS characterization of the swollen and shrunken states of IO-1 and IO-2 using Au-IDEs. The study explains that the impedance spectra, the diffusion rate of water through the polymer matrix and the swelling/drying process of IOs are linked to the influence of the IL on the morphology of the resulting ionogel. Monitor the structural integrity of the smart materials can help to detect many potential errors in the working performance of such devices.

## 2. Experimental

Au-IDEs were deposited onto oxidized silicon substrate by RF magnetron sputtering (Edwards coating system E306A). The Au layer were patterned using a polyester based mask with a finger width of 50 µm [7]. An average thickness of 200 nm was measured with a KLA Tencor pefilometer. Ionogels synthesis [8] were performed, using N-isopropylacrylamide, N,N'-methylene-bis(acrylamide) and (2,2-Dimethoxy-2-phenylacetophenone) dissolved in 1-ethyl-3-methylimidazolium ethyl sulfate (1) or trihexyltetradecyl-phosphonium dicyanamide (2) ILs. The chemical structure of the IOs used in this study are shown in Fig. 1. The IOs were in situ photopolymerized onto the Au-IDEs with UV light. Gaskets made of cycloolefin polymer (COP) and Pressure Sensitive Adhesives (PSA) were placed around the IDEs to contain the IO into the sensing area. EIS analysis were performed using a Hioki 5370 impedance analyser in the frequency range of 4Hz to 1MHz and applied amplitude of 2V. The data were fitted with an equivalent circuit using ZView to quantitatively analyse the results.

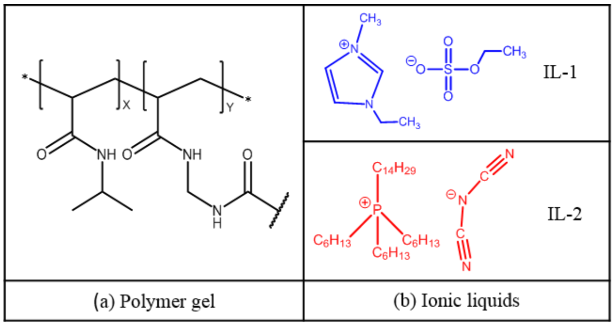


Fig. 1. Chemical structure of (a) polymer gel and (b) IL-1 and IL-2. The combination of (a) and (b) results in IO-1 and IO-2.

## 3. Results and discussion

EIS technique was used to understand the relationship of morphology and IOs polarity with the swelling behavior. Fig. 2 shows significant differences between the Nyquist diagrams of (a) IO-1 and (b) IO-2. The dominant process of the IO-1 is the Warburg diffusion ($Z_w$) while for IO-2 the main process is associated with the charge transfer resistance ($R_{ct}$). This can be related with the differences in polarity between IO-1 and IO-2. In particular the long-chain alkyl groups of $[P_{6,6,6,14}]^+$, which are responsible for the hydrophobic nature of IL-2, difficult the diffusion. The spectra were fitted with the Randles equivalent circuit that contains the following elements: IO resistance ($R_{IO}$), $R_{ct}$, constant-phase element (CPE) and $Z_w$ [9]. CPE-like behavior arises when the RC time constant is non-uniform over the surface of the electrode [10]. $R_{ct}$ values of 2,7 and 703,9 kΩ were obtained for IO-1 and IO-2, respectively.

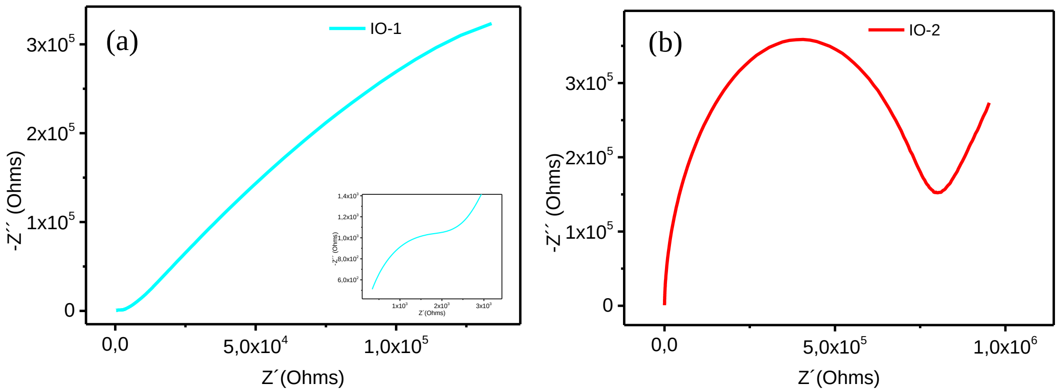


Fig. 2. Nyquist plot of (a) IO-1 and (a) IO-2 at 2V. The high frequency part of IO-1 spectra is detailed in the inset.

Sheet resistance is a parameter related with the quality assurance of conductive thin films. The parameter is related with the ability of IO-1 and IO-2 to resist current. The sheet resistance ($R_s$) was calculated using a two-point-probe and taking into account the dimensions of the IDEs. The $R_s$ values obtained were $1{,}87 \cdot 10^6$ Ω/sq and $8{,}08 \cdot 10^8$ Ω/sq at 1V for IO-1 and IO-2, respectively. As can be observed the $R_s$ of IO-1 is two orders of magnitude lower than for IO-2.

The diffusion of water passing through the IOs is related with the porosity and polarity of the matrix. To analyze this, the evolution of $Z_w$ with time after adding a water droplet was studied. The values listed in table 1 show that $Z_w$ of IO-1 decreases quicker than IO-2 values. According to the results, IO-1 exhibits a more open matrix with high cavities that are efficiently pre-disposed for water uptake and its hydrophilic anion allows for a faster diffusion of water through the polymer matrix. In contrast IO-2 has a compact surface with small cavities [2].

Table 1. Evolution of the Warburg factor for IO-1 and IO-2 at 2V at different times.

| Entry | t (s) | Zw (IO-1) | Zw (IO-2) |
|---|---|---|---|
| 1 | 0 | 1.84 | 0.139 |
| 2 | 20 | 0.795 | 0,125 |
| 3 | 40 | 0.231 | 0,114 |
| 4 | 60 | 0.3771 | 0,1 |
| 5 | 80 | $1{,}03 \times 10^{-2}$ | $8.964 \times 10^{-2}$ |
| 6 | 100 | $6{,}836 \times 10^{-3}$ | $8.113 \times 10^{-2}$ |
| 7 | 120 | $5.923 \cdot 10^{-3}$ | $6.517 \times 10^{-2}$ |

To characterize the swelling behavior of IO-1 and IO-2, different drying/swelling cycles were performed on the systems. The Nyquist plots of each step are showed in Fig. 3. It was observed that IO-1 suffers an easier recovery of its original characteristics considering that IO-2 needs longer immersion and drying times. This behavior could be explained because in IO-2 water molecules have slower diffusion and are trapped stronger inside the pores [8]. Moreover, the surface of IO-2 has a few pores with small diameter that results in a slow process. On the contrary, IO-1 presents a porous surface with a huge quantity of pores with different diameter. This results in a higher active surface with infinite routes for water uptake or release.

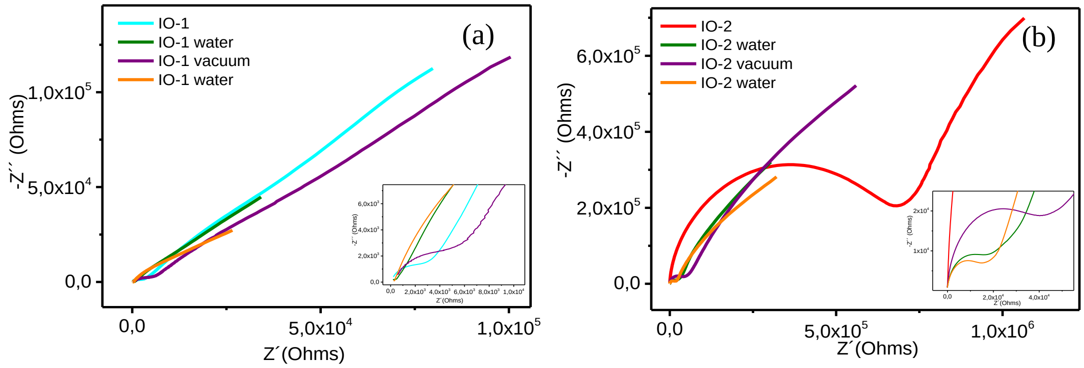


Fig. 3. Nyquist plot of (a) IO-1 and (b) IO-2 during swelling/drying cycles. The high frequency part of the spectra is detailed in the inset.

## 4. Conclusions

The interfacial properties of IO-1 and IO-2 were investigated by EIS. The hybrid material consists in pNIPAAM photopolymerized in the presence of two different ILs. It was found that the ILs entrapped within the polymer matrix have a significant influence on the impedance spectra of the IOs. The Nyquist plots show that the main process for IO-1 is the Warburg diffusion while for IO-2 charge transfer resistance. Water diffusion experiments together with the study of the swelling/shrinking behavior of the IOs conclude that the more porous surface of IO-1 and its hydrophilic nature are the main reasons for its more effective response. Finally, we have proved the use of EIS to seek the fundamental electrochemical processes of the polymer and provide new mechanistic insights into their behavior.

## Acknowledgements

This work was supported by the Basque Government under the Etortek Program (Grant No. IE14–391). N.G-G. was supported by a PhD fellowship from the University of Navarra.

## References

[1] F. Benito-Lopez, M. Antoñana-Díez, V. F. Curto, D. Diamond, and V. Castro-López, "Modular microfluidic valve structures based on reversible thermoresponsive ionogel actuators.," Lab Chip, vol. 14, no. 18, pp. 3530–8, 2014.
[2] M. Czugala, C. O'Connell, C. Blin, P. Fischer, K. J. Fraser, F. Benito-Lopez, and D. Diamond, "Swelling and shrinking behaviour of photoresponsive phosphonium-based ionogel microstructures," Sensors Actuators, B Chem., vol. 194, pp. 105–113, 2014.
[3] B. Ziolkowski, M. Czugala, and D. Diamond, "Integrating stimulus responsive materials and microfluidics: The key to next-generation chemical sensors," J. Intell. Mater. Syst. Struct., vol. 24, no. 18, pp. 2221–2238, 2012.
[4] A. Richter, D. Kuckling, S. Howitz, T. Gehring, and K. F. Arndt, "Electronically controllable microvalves based on smart hydrogels: Magnitudes and potential applications," J. Microelectromechanical Syst., vol. 12, no. 5, pp. 748–753, 2003.
[5] X. Z. Zhang, R. X. Zhuo, J. Z. Cui, and J. T. Zhang, "A novel thermo-responsive drug delivery system with positive controlled release," Int. J. Pharm., vol. 235, no. 1–2, pp. 43–50, 2002.
[6] B. Pejcic and R. De Marco, "Impedance spectroscopy: Over 35 years of electrochemical sensor optimization," Electrochim. Acta, vol. 51, no. 28, pp. 6217–6229, 2006.
[7] L. Rojo, I. Castro-hurtado, M. C. Morant-miñana, G. G. Mandayo, and E. Castaño, "Enhanced features of Li2CO3 induced by thickness and annealing time," CrystEngComm, vol. 17, pp. 1597–1602, 2015.
[8] T. Akyazi, J. Saez, J. Elizalde, and F. Benito-Lopez, "Fluidic flow delay by ionogel passive pumps in microfluidic paper-based analytical devices," Sensors Actuators, B Chem., vol. 233, pp. 402–408, 2016.
[9] T. Ito, K. Hosokawa, and M. Maeda, "Detection of single-base mismatch at distal end of DNA duplex by electrochemical impedance spectroscopy," Biosens. Bioelectron., vol. 22, no. 8, pp. 1816–1819, 2007.
[10] B. A. Yezer, A. S. Khair, P. J. Sides, and D. C. Prieve, "Use of electrochemical impedance spectroscopy to determine double-layer capacitance in doped nonpolar liquids," J. Colloid Interface Sci., vol. 449, pp. 2–12, 2015.